Metallic and nonmetallic shine in luster: An elastic ion backscattering study

T. Pradell, A. Climent-Font, J. Molera, A. Zucchiatti, M. D. Ynsa et al.

Additional information on J. Appl. Phys.

Metallic and nonmetallic shine in luster: An elastic ion backscattering study

T. Pradell[a)]
Departament Física i Enginyeria Nuclear, Universitat Politècnica de Catalunya,
Campus Baix Llobregat. ESAB. Av. Canal Olímpic, 08860 Castelldefels, Spain

A. Climent-Font
Centro de Micro-Análisis de Materiales, Universidad Autónoma de Madrid, Campus de Cantoblanco,
28049 Madrid, Spain and Departamento de Física Aplicada, C-XII, Universidad Autónoma de Madrid,
Campus de Cantoblanco, 28049 Madrid, Spain

J. Molera
GRMT, Departament, Física, Universitat de Girona, Campus Montilivi, 17071 Girona, Spain

A. Zucchiatti
Departament di Fisica, Università di Genova, e INFN via Dodecaneso 33, 16146 Genova, Italy

M. D. Ynsa
Centro de Micro-Análisis de Materiales, Universidad Autónoma de Madrid, Campus de Cantoblanco,
28049 Madrid, Spain

P. Roura
GRMT, Departament Física, Universitat de Girona, Campus Montilivi, 17071 Girona, Spain

D. Crespo
Departament Física Aplicada, Universitat Politècnica de Catalunya, Campus Baix Llobregat.
EPSC. Av. Canal Olímpic, 08860 Castelldefels, Spain

Luster is a metal glass nanocomposite layer first produced in the Middle East in early Islamic times (9th AD) made of metal copper or silver nanoparticles embedded in a silica-based glassy matrix. These nanoparticles are produced by ion exchange between Cu^+ and Ag^+ and alkaline ions from the glassy matrix and further growth in a reducing atmosphere. The most striking property of luster is its capability of reflecting light like a continuous metal layer and it was unexpectedly found to be linked to one single production parameter: the presence of lead in the glassy matrix composition. The purpose of this article is to describe the characteristics and differences of the nanoparticle layers developed on lead rich and lead free glasses. Copper luster layers obtained using the ancient recipes and methods are analyzed by means of elastic ion backscattering spectroscopy associated with other analytical techniques. The depth profile of the different elements is determined, showing that the luster layer formed in lead rich glasses is 5–6 times thinner and 3–4 times Cu richer. Therefore, the metal nanoparticles are more densely packed in the layer and this fact is related to its higher reflectivity. It is shown that lead influences the structure of the metal nanoparticle layer through the change of the precipitation kinetics. © *2007 American Institute of Physics.*
[DOI: 10.1063/1.2734944]

I. INTRODUCTION

Luster is a metal glass nanocomposite layer made of metal copper or silver nanoparticles embedded in a silica-based glassy matrix. The metal particles range from 2 to 50 nm size and the whole layer is from 100 nm to about 1 μm thick.[1–5] Luster was discovered in the Middle East in early Islamic times (Iraq, 9th AD) when the ceramists learned the physical-chemical mechanisms involved in luster formation.[6]

The luster technique is very complex and includes ion exchange between Cu^+ and/or Ag^+ and alkaline ions from the glassy matrix (Na^+ and K^+), diffusion of the metal ions followed by nucleation, and growth in a reducing atmosphere to form metal copper and/or silver nanoparticles in the glass.[7–9]

The materials and firing procedures used should be so carefully controlled that it is highly surprising that 9th AD potters managed to control the process so well, considering their limited scientific and technical knowledge.

The optical properties of the luster layers are determined by the nature of the metal nanoparticles and size distribution, their volume fraction, the thickness of the layer, and the composition of the glassy matrix.[10] In particular, their color (typically red, brown, green, yellow, and amber) depends mainly on the nature and size of the metal nanoparticles (Cu and/or Ag) and the presence of ions (Cu^+ and Cu^{2+}) dissolved in the glass structure.[11–13] In addition, one of the most striking properties of luster is its capability of reflecting light like a metal surface. For example, a green luster layer may show a gold-like shine,[6] but it is also possible to have a dark

a)Electronic mail: trinitat.pradell@upc.edu

brown luster showing also a gold-like shine.[6] Therefore, the color observed under diffuse light is different from the color observed under reflected light. The increase in the reflectivity of the layer is related to the transition from individual cluster Mie scattering (electromagnetic interaction of incident light with individual spherical particles) toward the regularly transmitted and reflected beams of geometrical optics which are explained in terms of the Fresnel equations. This change from single particle to collective behavior shown by dense cluster films, is known as the Oseen effect, explained by the Ewald–Oseen theory and evaluated by Torquato–Kreibig–Fresnel model (TKF model).[14] The Oseen transition from incoherent scattering into geometric-optical transmission and reflection is due mainly to the interference among the scattered electromagnetic waves of all particles.[15] Actually, the high reflectivity shown by these layers is known to be nanoparticle size and volume fraction (f) dependent.[14]

Recently, laboratory reproductions of medieval luster using a medieval recipe[16] found during the excavations of the 13th century AD Paterna (Valencia, Spain) workshop were performed.[8,9] Several thermal paths and atmospheres (oxidizing, neutral, and reducing), luster formulas and glaze compositions were checked in order to reproduce the colors and shines of medieval lusters. Green-yellow and green-yellow golden lusters, as well as red ruby and red coppery lusters were obtained using either silver or copper containing recipes.[9] Brown, dark brown, amber, and orange lusters were obtained using a mixed copper and silver containing recipe.[17] Although luster layers were obtained in the whole range of temperatures checked (450 up to 600 °C), optimal lusters were obtained at temperatures of 550 °C. The need of combined oxidizing/neutral followed by reducing thermal path was demonstrated. During the oxidizing/neutral stage the ionic exchange between the luster paint and the glaze was obtained; in the subsequent reducing process the reduction to metallic state of the Cu^+ and/or Ag^+ introduced in the glaze was obtained.

The analysis of the layers showed that, depending on the glaze composition, the size of the nanoparticles was different, being smaller for the lead free glazes. However, the total Cu/Ag content of the luster layers was similar in all the cases, provided that similar firing times were used for the first neutral/oxidizing stage when the ionic exchange took place.[8,9]

The composition of the glaze was found to be strikingly important. Luster layers produced on lead free glaze never showed metallic shine, conversely luster layers obtained on lead containing glazes (32% PbO) do exhibit a metallic shine.

Moreover, these studies[8,9] demonstrated that for lead-free glasses the luster layers produced at higher temperatures (up to 600 °C), and longer reducing times (10–20 min) show a similar, but more intense, color. The size of the nanoparticles increases and the total amount of Cu/Ag increases with increasing temperature and reducing time but the metal shine is not achieved. On the contrary, for the lead glaze the metal shine is always obtained provided that temperatures of 550 °C are reached, even for shorter reducing times (5 min).

One possible explanation for this behavior is the presence of a higher volume fraction of metal nanoparticles in the layer.

The object of the present study is to determine the chemical composition metal volume fraction and thickness of the copper luster layers obtained on lead free and lead containing glasses/glazes.[8,9] Elastic ion backscattering spectroscopy (EIBS), also known as Rutherford backscattering spectroscopy, allows the evaluation of the elemental composition of a layered structure that is a few microns thick, and in particular it may provide thickness and elemental composition of the copper luster layers. This information is processed to determine the volume fraction of metal nanoparticles in the luster layer (f). The differences in composition between the copper luster layers produced on lead free and lead containing glazes are compared. The results are discussed to explain the presence or otherwise of metallic shine. The role of lead in the formation of metal shining luster layers is also discussed.

II. MATERIALS AND TECHNIQUES

Chemical analyses were obtained by electron microprobe, using a Cameca S-50 (WDX) instrument. Experimental conditions being 1 μm spot size, 15 kV and 10 nA probe current except for Na and K for which the probe current was reduced to 1 nA and the spot size increased to about 5 μm. Synchrotron radiation x-ray microdiffraction (SR-Micro-XRD) was performed at SRS Daresbury Laboratory in transmission geometry, 0.87 Å wavelength, 200 μm spot size, and recorded in a charge coupled device detector and also in reflection geometry 1.4 Å wavelength, 1 mm spot size, and 0.01° step size, details are given elsewhere.[8,9]

EIBS measurements were made with the 5 MV tandem accelerator at CMAM.[18] The analysis were performed in vacuum using a 3035 keV He beam in order to take advantage of the elastic resonance $^{16}O(\alpha, \alpha)^{16}O$ occurring at this energy[19] and which increases the sensitivity to detect oxygen by a factor of 23. The size of the beam was a square of 1 mm diagonal. The backscattered ions were analyzed by means of two particle surface barrier detectors, one fixed at 170° scattering angle and a mobile one, whose scattering angle can be varied, which was set at 165°. Normally the two detectors are currently used as a double check for the EIBS spectra obtained. When elastic resonance happens, the choice of the scattering angle of the mobile detector is determined from scattering angles and scattering cross sections available database. A careful quantification of the EIBS spectra was achieved using the simulation code SIMNRA.[20]

The luster layers were obtained as described in Refs. 8 and 9 by applying a synthetic raw luster mixture containing 60% illitic clay, 10% CuO, and 30% HgS selected after the archeological findings in the site excavations from the 13th century AD Paterna workshop.[16] Historically, luster nanolayers were developed over glasses and glazed ceramics. Therefore, three different glasses and glazes were selected: a lead glaze (glaze-m) applied over a white ceramic substrate, a high Na content lead free glaze (glaze-a) which was also applied to a white ceramic substrate, the final example was actually a lead free glass coverslip from Marienfeld (glass-a).

TABLE I. at. % composition of the glass/glazes determined by electron microprobe and EIBS analysis of the surface.

at%	ID	Si	Na	K	B	Al	Pb	Ca	Mg	Zn	Sb	Ti	O
Lead free glass	Glass-a	22.1	4.4	2.8	4.9	1.7	⋯	⋯	⋯	1.5	0.07	1.1	61.5
Lead free glaze	Glaze-a	15.3	6.6	3.2	12.6	2.7	<0.065	0.5	0.05	0.1	⋯	⋯	58.9
Lead glaze	Glaze-m	20.1	3.5	2.0	7.0	3.2	4.0	0.5	0.2				59.5

The chemical composition measured by electron microprobe analysis and EIBS directly from the surface of the glass and glazes are given in Table I. Glaze-a is not fully lead free, but it contains a very small amount of PbO (<0.4 wt %). The luster raw mixture was applied over the glazes surface and then fired in a small furnace under controlled conditions. The firing protocols included a heating rate of 50 °C/min and 20 min dwell time in neutral atmosphere (Ar), switching to a reducing atmosphere consisting of a mixture of 5% H_2 and 95% N_2, 5 or 10 min dwell time at the maximum temperature, and free cooling.

Although it is well established that EIBS is a convenient technique to obtain composition depth profiles,[21] it has not been used until rather recently to determine such profiles in luster ceramics.[4,5,22–24]

III. RESULTS

The luster layers and some relevant data obtained from their analysis are shown in Fig. 1.[9] The three luster layers were obtained using the same production parameters, except that the length of the reducing time for the lead containing glaze (glaze-m), which was reduced to 5 min instead of 10 min. The use of a shorter reducing time also produced a good luster, which was actually of better quality. The use of a highly reducing atmosphere with lead glazes may result in the reduction of the lead to metal and a slight darkening of the glaze surface; indeed the luster obtained after 10 min showed some darkening while the luster reduced for 5 min

(j65) did not apparently show this darkening. This is the reason why the luster prepared with lower reducing time was preferred for this study.

As shown in Fig. 1, the luster layers obtained on the lead free glass (j32) and lead free glaze (j6) showed a red ruby color and no metallic shine. On the contrary, the luster layer produced on the lead glaze (j65), did show a full coppery shine, like a metal copper film.

Chemical analysis of the luster layers was obtained by electron microprobe analysis of the luster surface as described in Refs. 8 and 9. Considering the density and composition of the glazes, the penetration depth of the electron microprobe as determined from the Kanaka–Okayama range is of about 3 μm, thus the obtained chemical composition is averaged over a region several times larger than the luster layer itself. The data given in Fig. 1 are the average and standard deviation (shown in brackets) of at least 15 measurements taken at different points of the luster. The total amount of copper is similar for the three lusters.

Chemical analysis of the luster layers demonstrated that the incorporation of copper into the glaze surface was obtained by ionic exchange of the Cu^+ ions from the raw luster paint with the Na^+ and K^+ ions from the glaze.[8,9] Figure 2 shows the linear characteristic correlations obtained when plotting the atomic concentration of Cu vs K and Na.

The nature and size of the nanoparticles was determined by SR-Micro-XRD and is also given in Fig. 1; the particle size was obtained from the peak width by peak profile analysis of the diffraction peaks from measurements taken on dif-
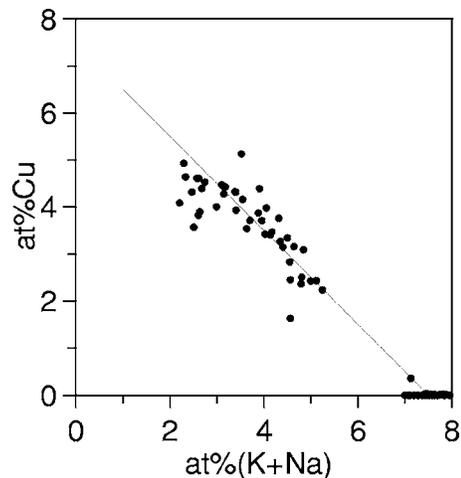
Sample Id.	J32	J6	J65
	(a)	(b)	(c)
Glass type	Glass-a	Glaze-a	Glaze-m
Glass density (g/cm³)¹	2.42	2.32	3.01
wt% PbO in glass	0	0.4	32
Average & standard deviation (at%Cu)²	3.4(1.4)	2.6(1.2)	1.8(1.2)
Maximum (at%Cu)²	4.8	4.3	4.0
Size of nanoparticles (nm)³	6.4(0.3)	12.5(0.3)	39.0(3.1)

FIG. 1. Summary of the main characteristics of the luster layers studied.[1] Calculated from the glazes composition following Ref. 26.[2] Values for the luster surface as determined by electron microprobe analysis. The data are the average of at least 15 measurements and the standard deviation is given between brackets. The penetration depth of the electron microprobe determined from the Kanaka–Okayama range is of about 3 μm and therefore this value is the average composition of a region several times larger than the luster layer itself.[3] Metal copper and cuprite nanoparticles were determined in all the cases and the size of the nanoparticles was calculated from peak width analysis of SR Micro-XRD data (see Ref. 8).

FIG. 2. Electron microprobe analysis of the surface of the lead free glass luster (j32) and of the luster lead free glass (glass-a). The depletion in Na and K in the layer is related to the increase in Cu.

ferent areas of the samples as described in Refs. 8 and 9. In all the cases metal copper nanoparticles were determined and, in some of the measurements, a small amount of cuprite was also determined. The size of the metal nanoparticles increases from 6.4±0.3 nm for the lead free glass luster (j32) and 12.5±0.3 nm for the lead free glaze luster (j6) up to 39.0±3.1 nm for the lead glaze luster (j65). In particular, extended x-ray absorption fine structure (EXAFS) and transmission electron microscopy (TEM) analysis of a luster layer prepared following the same thermal protocol on the lead free glaze, thus equivalent to j6, has been recently performed.[25] The size of the nanoparticles fully matches the size obtained by SR-Micro-XRD; the luster layer has a higher density of nanoparticles in a sublayer of about 800 nm thickness and has a copper free outer layer of about 50 nm. EXAFS data determined 77±4% copper metal, with the remainder as the cuprite. Whether the cuprite is attached to the nanoparticles or just dissolved in the glassy matrix is unclear. SR-Micro-XRD analysis of the luster layers indicates the presence of some crystalline cuprite. Similar results have been found for medieval lusters.[4,11–13]

EIBS analysis of both the glaze luster free surface and the luster layers have been performed for the three glaze compositions and corresponding luster layers, and are shown in Figs. 3–5, respectively, and the corresponding composition depth profiles are shown in Fig. 6. The spectrum corresponding to the lead free glass is simulated using the chemical composition given in Table I and considered constant over the whole depth analyzed. The agreement between simulated and experimental spectra is excellent as can be seen in Fig. 3(a). The high energy edges for the signal corresponding to the fitted elements are marked in the figure. It should be mentioned that for light elements, B, Na, K, the sensitivity of EIBS is very low (±1%), so it may be meaningless for this element to give percent concentration values with decimal figures. However, as the code SIMNRA accepts inputs for the atomic concentrations normalized to unity, giving precise values to the concentrations for the heavier elements, for which the sensitivity of EIBS is high, necessarily imposes values for the light elements with figures beyond the significant values.

During the luster production, the glass has to be heat treated to 550 °C under neutral and then reducing atmospheres. This process could affect the chemistry of the glass surface. Both the EIBS spectrum corresponding to the untreated glass (no heat treatment) and the heat-treated glass are shown in Figs. 3(a) and 3(b) and are compared to the simulated EIBS spectrum using the nominal chemical composition of the lead free glass (Table I). The good agreement in the fit of both spectra indicates that, up to the EIBS sensitivity, no appreciable changes in composition are induced in the glass surface by the heat treatment.

The experimental and simulated EIBS spectra corresponding to the lead free glass luster layer, j32, are shown in Fig. 3(c). Incorporation of Cu in the luster process is observed in the region between channels 600 and 900. The EIBS spectrum reveals that it has a complex chemical depth profile. The simulation of this profile was performed by using a set of successive layers (up to 9), where the atomic
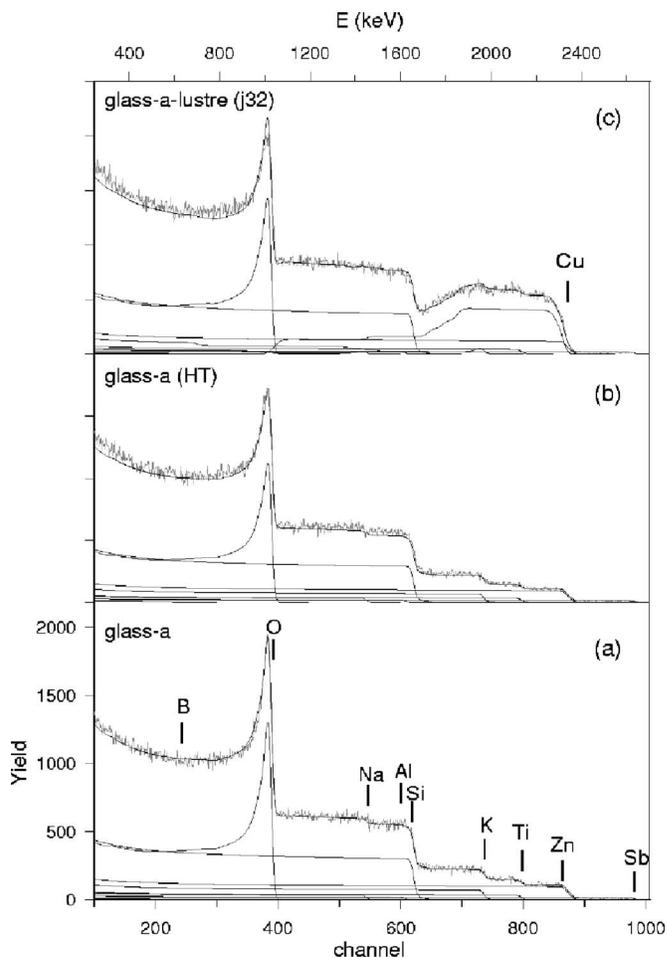

FIG. 3. EIBS experimental (gray line) and simulated spectra (black line) and the contribution of the different elements corresponding to (a) lead free glass (glass-a), (b) lead free glass heat treated (glass-a HT) following the same thermal protocol used during the luster production, and (c) luster developed on lead free glass (j32). The incorporation of Cu in the luster process is observed in the region between channels 600 and 900.

percent concentrations for all elements other than Na, K, and Cu were kept constant. According to the correlations shown in Fig. 2, we assumed that each Cu atom entering the glass removes an atom either of Na or K. The thickness of the layers is defined in the units pertinent to EIBS, i.e., areal density in units of 10^{15} at/cm². The areal density can be transformed into a depth provided that the composition and the density of the material is known through the relationship, depth=areal density(at/cm²)/density(at/cm³). For our glasses and glazes the composition is known and the density may be estimated from their composition using the expressions given in Ref. 26, the resulting densities for the three glazes are also given in Table I. Taking a density of 2.42 g/cm³ for the lead free glass, areal density of 10^{15} at/cm² is equivalent to a depth of 1.43 Å. Figure 6(a) shows the resulting chemical profile concentration obtained from the fits of the EIBS spectrum.

The values for the Cu content in the plateau region (between 1000×10^{15} and 7000×10^{15} at/cm²—equivalent to 0.14 and 1 μm depth) are very reliable, with an accuracy well below 1%. For layers above 8000×10^{15} at/cm² (about 1.14 μm depth), the Cu concentration determined is less ac-
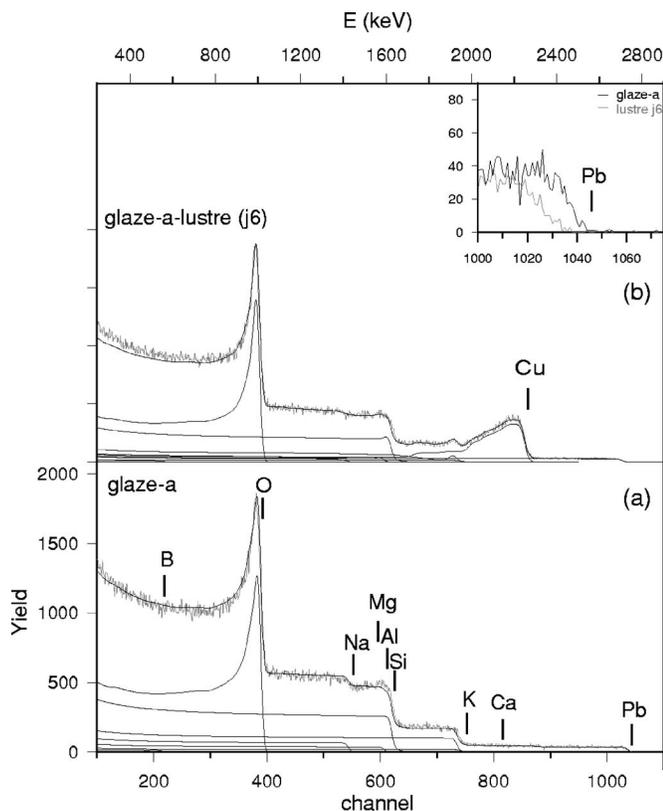
FIG. 4. EIBS experimental (gray line) and simulated spectra (black line) and the contribution of the different elements corresponding to (a) lead free glaze (glaze-a) and (b) luster developed on lead free glaze (j6). The incorporation of Cu in the luster process is observed in the region between channels 750 and 850. The inset enlarges the region between channels 1000 and 1075 corresponding to the contribution of lead to the spectrum; it can be clearly seen that the surface layer is lead depleted.

curate as can be seen in Fig. 3(c) (channels below 730). In the region between channels 640 and 730 the Cu signal still does not overlap with the Si signal so accuracy below 1% can still be obtained. However, when the Cu signal overlaps with the Si signal, below channel 630, the uncertainty may
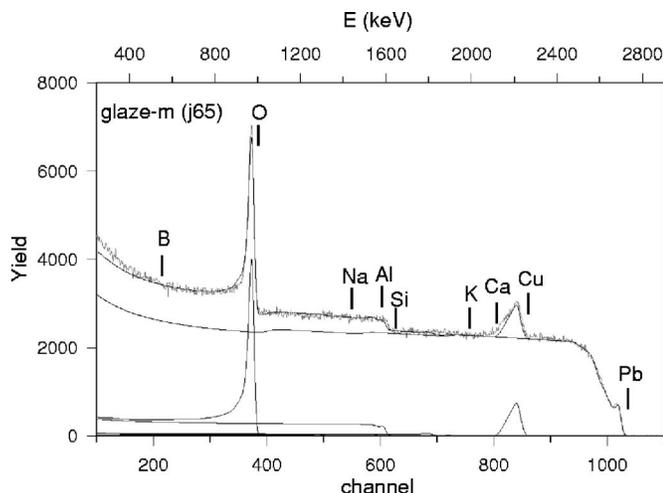

FIG. 5. EIBS experimental (gray line) and simulated spectra (black line) and the contribution of the different elements corresponding to luster developed on lead glaze (j65). The incorporation of Cu in the luster process is observed in the region between channels 800 and 850.
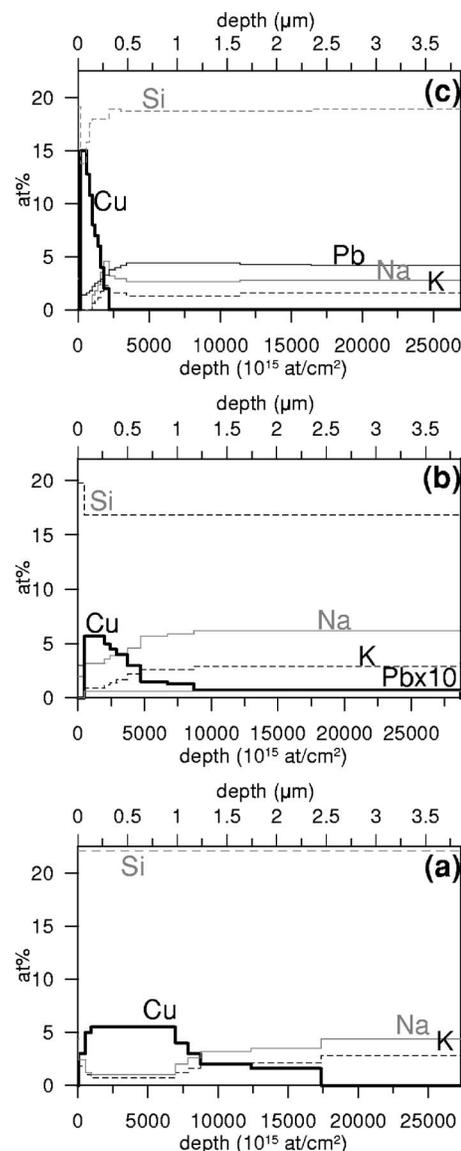

FIG. 6. Elemental profile concentration obtained from the EIBS data for the three luster layers (a) lead free glass luster—j32, (b) lead free glaze luster—j6, and (c) lead glaze luster—j65.

be considerably higher. In our simulation the Cu free region starts at a depth $17\,350 \times 10^{15}$ at/cm^2 (about 2.5 μm depth).

The assumed changes in the concentration values for Na and K are less accurate than for Cu. The K signal overlaps with the Cu and Zn signals which have an important contribution to the total spectrum and the Na signal overlaps with the Si signal. In the simulation we have decided to keep the K/Na ratio roughly constant in the region where Cu is present.

Finally, the average copper composition calculated from the EIBS results up to a depth of 3 μm, is 2.8 at. % Cu while the average copper concentration determined by electron microprobe gives a value of 3.4(1.4) at. % Cu.

We can summarize the main results obtained for the lead free glass luster (j32) as follows:

(1) There is a surface layer with a thickness of 50×10^{15} at/cm^2 (about 7 nm) free of Cu.
(2) The shape of the Cu profile in the lead free glaze luster

layer j32 is asymmetric, showing a sharp increase at the boundary between the copper free outer layer and the copper containing inner layer and more gradual decrease inside. The region with a high Cu concentration has a thickness of about 8000×10^{15} at/cm^2 (1.1 μm).

The EIBS spectra from the lead free glaze and from the corresponding luster, j6, are shown in Figs. 4(a) and 4(b). As for the lead free glass, EIBS gives homogeneous and similar compositions for the untreated glaze and for the heat treated glaze and are given in Table I. The peak related to the presence of Cu is clearly seen in Fig. 4(b). The shape of the peak indicates a sharp rise in the Cu content going deeper into the glaze surface, followed by a small and gradual decrease which may reach several microns in depth. A good fit to the experimental data is obtained, as shown in Fig. 4(b), using ten layers where relative concentrations of Si, Na, K, Cu, and Pb are modified while those of the other elements remain constant. Taking a density of 2.32 g/cm^3 for the lead free glaze,[26] an areal density of 10^{15} at/cm^2 is equivalent to 1.34 Å. The concentrations and thickness of the simulated layers are shown in Fig. 6(b). Again, the amount of Cu is kept equal to the total loss of Na and K. The glaze contains a small amount of Pb (0.065 at. %) which can be easily and precisely detected by EIBS due to the high atomic number of Pb. The inset in Fig. 4(b) shows that a layer close to the surface is Pb depleted, due to the volatilization of Pb during the luster production; this has already been observed in the literature.[24] In the region of channels higher than 870 (corresponding approximately to a depth of about 1.2 μm), the lead signal begins to overlap with the Cu signal, and the lead content cannot be well determined. The average copper composition calculated for different samples for a depth of 3 μm ranges from 1.5 to 2.6 at. % Cu which is in excellent agreement with the average copper concentration determined by electron microprobe 2.6(1.2) at. % Cu.

We can summarize the results obtained for lead free glaze luster (j6) as follows:

(1) There is a surface layer free of Cu of 500×10^{15} at/cm^2 thickness (about 67 nm). This layer is also Pb free and Si richer.
(2) The shape of the Cu profile in the lead free glaze luster layer j6 is asymmetric, showing a sharp increase at the boundary between the copper free outer layer and the copper containing inner layer and more gradual decrease inside. The Cu rich layer has 4200×10^{15} at/cm^2 (about 560 nm) thickness.

Both results correspond very well with the TEM image from the luster layer obtained using the same thermal protocol on lead free glaze.[25]

The EIBS experimental spectrum and fit corresponding to luster layer j65 developed on the lead glaze is shown in Fig. 5 The glaze is lead rich and contains 4 at. % of Pb (corresponding to 32 wt % PbO). The presence of high amounts of Pb limits the accuracy of EIBS to measure the depth profile concentrations of the elements lighter than lead. Fig. 5 shows a sharp Cu asymmetric peak overlapping the Pb signal. The concentrations and thickness of the simulated

layers are shown in Fig. 6(c). Taking a density of 3.01 g/cm^3 for the lead glaze,[26] an areal density of 10^{15} at/cm^2 is equivalent to 1.43 Å. The luster layer is Pb depleted with respect to the nominal composition as can be clearly observed in the EIBS spectrum. The EIBS spectrum shows that, in this case, the luster layer has a very thin copper rich region, 1000×10^{15} at/cm^2 (about 140 nm) thick. This results in a high copper nanoparticles volume fraction, higher than 10%. Therefore, there is a significant reduction in the glass volume fraction and consequently in the Si content of the layer. The EIBS simulation indicates that the depletion in Na, K, and Pb reaches a deeper region. However, the sensitivity of EIBS to these elements is heavily limited in this high lead containing glaze and the glaze composition determined, must be considered with caution. The Si enriched and Pb depleted surface layers have also been observed in the study of ancient lusters.[5,24] The average copper composition calculated for a depth of 3 μm, is 0.8 at. % Cu while the average copper concentration as determined by electron microprobe is 1.8(1.2) at. % Cu.

A summary of the analysis for lead glaze luster layer (j65) indicates:

(1) The presence of a Cu free outer surface layer of a thickness 200×10^{15} at/cm^2 (about 28 nm). This layer is also Si richer and Pb poorer than the glaze, although richer in Pb than the Cu containing region.
(2) The Cu concentration profile is asymmetric, showing a sharp rise up to a maximum concentration much greater (15 at. %) than in the previous cases, followed by a smooth decrease but which is sharper than in the previous cases. The Cu rich luster layer is 1000×10^{15} at/cm^2 (about 140 nm) thick.

A comparison between the three luster layers studied shows some similarities: the presence of a copper free outer layer, the concentration of copper in a thin layer showing an asymmetric profile, steeper near the surface and smoother inside the glaze. There are also some differences: the lead glaze has a luster layer 5–6 times thinner (only 140 nm thick) and a copper concentration 3–4 times larger (10–15 at. %) than the other glazes. Moreover, the lead glaze has also bigger copper nanoparticles, 39.0±3.1 nm in front of 6.4±0.3 nm for the lead free glass luster (j32) and 12.5±0.3 nm for lead free glaze luster (j6) (as shown in Fig. 1).

IV. DISCUSSION

The copper content in the luster layer as obtained from EIBS allows us to calculate the volume fraction of copper nanoparticles -*f*- (taking a density of 8.9 g/cm^3 for copper and the corresponding density given in Table I for each glaze). EXAFS data for a lead free glaze luster (similar to j6), a luster layer produced following the same thermal protocol[25] showed that 77±4% of the copper was in metallic state while the rest was a cuprite. However, it is also well known that due to the fact that the reducing process results from the penetration of the reducing atmosphere into the luster layer, the outer surface is always more reduced than

TABLE II. Copper and glass weight fractions calculated from the EIBS data and copper volume fraction (f). The mean interparticle distance ratio (D/d) between copper particles is calculated from f considering a random arrangement of nanoparticles using the exact solution given in Ref. 27.

Glaze	Luster ID	% of metal copper	Cu (wt %)	Glass (wt %)	f (%)	D/d
Lead free glass	j32	100	15.4	84.6	4.7	1.43
		80			3.8	1.50
Lead free glaze	j6	100	17.4	82.6	5.2	1.39
		80			4.2	1.47
Lead glaze	j65	100	34.7	65.3	15.2	1.14
		80			12.2	1.18

the inner region of the luster layer. In the calculation we have considered both cases: either all the copper is forming metal nanoparticles or only 80% of the copper is forming metal nanoparticles. The calculated weight percent of copper and volume fraction for the copper richest regions of the three luster layers analyzed are presented in Table II which shows that the lusters developed on lead free glazes (j32 and j6) have values of $f \sim 5\%$ and the luster developed on the lead glaze (j65) has a larger value, $f \sim 15\%$.

We have also computed the average nearest-neighbor distance between the particles, which is given by the interparticle distance ratio D/d,[27] where D is the separation between centers of adjacent particles and d is the particle size. This parameter has been used to study the insulator-metal transition in metal nanoparticulated systems.[28] D/d is more suited for the study of dense nanoparticulated systems than the volume fraction, because the multipolar interaction is determined by the particle size and the nearest neighbor distance. Furthermore, for a given particle arrangement [face-centered-cubic, body-centered-cubic, simple-cubic (sc), or randomly arranged in three dimensions (3D), and triangular or randomly arranged in two dimensions (2D)] both f and D/d are directly related, and D/d can be calculated exactly from f and a given particle arrangement using the exact solution given by Torquato.[27] It is also worthwhile noting that the use of D/d allows a comparison of the observed response to other two-dimensional (2D) and three-dimensional (3D) nanoparticulated systems already studied in the literature. Considering that TEM images corresponding to both ancient luster layers and to the luster layer equivalent to lead free glaze luster (j6) (Refs. 1–5 and 25) always show a random arrangement of nanoparticles, we have calculated the interparticle distance ratio (D/d) using the exact relationship between f and D/d given by Torquato.[27] The results are also shown in Table II. Typical values of $D/d \sim 1.4$ are obtained for the lead free glazes lusters (j32 and j6) while a value below 1.2 is obtained for the lead glaze luster (j65).

Using the TKF model, Farbman *et al.*[14] calculated the reflectance of 3D concentrated metal nanoparticulated systems, showing that their reflectance increases with both particle size and volume fraction up to values similar to metal thin layers. They also concluded that a system with a lower volume fraction, but larger particles has a similar reflectance to a system with a larger volume fraction but smaller particles. Volume fractions above 10% ($D/d = 1.2$ for randomly arranged arrays) and particle sizes between 2 and 50 nm were considered. They reported also that reflectance depends on the spatial arrangement, being highest for sc and random arrangements. These calculations indicate that for 3D systems an increase in the reflectance is obtained when reducing D/d. They also observed that there is an increase in the reflectance with the dielectric constant of the matrix. Silver and gold were found to give higher reflectance than copper for equivalent particle size and volume fractions. Shiang *et al.*[28] studied the optical behavior of 2D arranged monolayers of 3 nm diameter silver nanoparticles both theoretically and experimentally. Their study showed that there is an increase in the reflectance of the layers for $D/d < 1.7$ and a reversible quantum insulator to metal transition for values of $D/d < 1.2$. The experimental data [metal reflectance, absorption and second order harmonic generation (SHG)] did not agree with the theoretical classical calculations. As a consequence, they concluded that quantum effects had to be taken into account to explain the high values of the reflectance and SHG determined when this transition happens. Quantum effects were expected in this case because the distance between near neighbor particles surfaces, $D - d = 6$ Å, was small enough. However, quantum effects are not expected in the luster layers studied here as, in all cases, the distance between particles surfaces is well above the nanometer.

Recently, Reillon and Berthier[29] analyzed medieval silver luster layers showing a gold metal shine and modeled its reflectance, reproducing qualitatively some of the most remarkable features shown by the layers. The lack of quantitative agreement with the experimental data was related to the complex structural features of the luster layers. Computations were performed assuming a 10% volume fraction ($D/d = 1.22$) of silver nanoparticles, radius 5, 10, and 20 nm and a dielectric constant of 2.

In our study, of the three luster layers studied, only the lead glaze luster layer has a D/d value below 1.2 (Table II). Luster developed over lead free glazes (j32 and j6) have values of $D/d \sim 1.4$. Therefore, we find here a change in the optical reflectivity of the layer from nonmetallic to metallic for D/d below 1.2, in good agreement with the literature.

The formation of a thinner copper rich luster layer when a lead rich glaze is used is responsible for the high reflectivity shown by the luster layer through the reduction of D/d. This may be related to a smaller diffusion of Cu^+ in the glaze after ionic exchange took place and prior to the copper reduction and formation of the metal nanoparticles. This reduced diffusivity may be a consequence of either a lower solubility of Cu^+ in the lead glaze or to a more complex diffusion path involving other elements from the glaze. Further studies are needed to clarify this question.

In any case, it has been established that the introduction of lead in the glaze formulation is fundamental in order to obtain a good metal like luster decoration. Actually, the glazes related to the earliest luster production, 9th AD (Iraq), contained only very low amounts of lead (1–5 wt % PbO) and the corresponding luster layers did not show metal-like
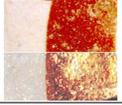
Sample ID	P37	P32	PRaqqa	Salt-11
	Iraq 10thAD	Iraq 10thAD	Syria 13thAD	Barcelona 17thAD
Metal shine	No		No	
Luster* (wt%)	3.4(1.3) Ag 0.08(0.04) Cu	4.0(1.0) Ag 0.4(0.1) Cu	6.4(0.9) Cu 0.07(0.03) Ag	1.9(0.5) Cu 0.9(0.3) Ag
PbO Glaze (wt%)	5.6(0.7)	14.9(0.6)	0	40.9(1.3)

FIG. 7. Early Islamic luster from the Ashmolean Museum (Oxford) and the 17th AD Barcelona luster from Salt (Girona). For the metal shinning lusters a picture taken changing the surface orientation to 45° to capture the reflected light is also shown.* The elemental composition of the luster layers was evaluated as described in Fig. 1.

shine.[6,29,30] Later (late 9th and 10th century AD), the introduction of higher amounts of lead in the glaze (up to 15 wt % PbO) resulted in the formation of gold-like silver lusters. Figure 7 shows two samples from the Ashmolean Museum— P37 and P32—with the characteristic green silver lusters from early 10th AD, Iraq.[6] The lack of golden like shine for sample P37 is clearly linked to the low lead content of the glaze unlike P32. Later luster productions from Egypt (Fustat, 10th–11th AD), Iran (Kashan, 12th–13th AD), Syria (12th), Islamic (Malaga, 13th century AD), and Christian Spain (Paterna 14th century AD) included lead in the formulation of the glazes (between 20 and 45 wt % PbO). There is only one exception in the Islamic luster productions, the copper luster layers produced in Raqqa, Syria, in the 13th AD (Ref. 6) that were obtained over pure alkaline glazes. In perfect agreement with our results these copper lusters are a red color and never show metallic shine (Fig. 7, sample Praqqa). On the contrary, coppery lusters were always obtained on high-lead containing glazes, as is observed in a typical luster from 17th century AD Barcelona (Fig. 7, sample Salt-11).

V. CONCLUSIONS

An EIBS study of copper luster layers produced in laboratory conditions using the medieval recipes with both lead-free and high lead glazes (32 wt % PbO) has been performed. Analysis of EIBS data gave the thickness and copper content of the luster layers from which the metal particle volume fractions and D/d were obtained. The results indicate that the metal-like reflectivity shown by the luster layer produced on the high lead glaze is related to a high density of particles in the layer and bigger nanoparticles size ($D/d \sim 1.2$), while the lack of metal shine of the luster layers produced on lead free glazes is related to a lower particle density and nanoparticles size (higher D/d).

The use of lead rich glazes seems one of the relevant technological parameters for the production of metal-like shining lusters. The study of early Islamic lusters agrees with this.[6,30] The results obtained in this article suggest that the

evolution of the luster technology during 9th and 10th centuries AD is directly related to the introduction of lead in the glaze formulation.

[1] J. Pérez-Arantegui *et al.*, J. Am. Ceram. Soc. **84**, 442 (2001).
[2] I. Borgia *et al.*, Appl. Surf. Sci. **185**, 206 (2002).
[3] J. Pérez-Arantegui, A. Larrea, J. Molera, T. Pradell, and M. Vendrell, Appl. Phys. A: Mater. Sci. Process. **79**, 235 (2004).
[4] S. Padovani *et al.*, J. Appl. Phys. **93**, 10058 (2003).
[5] D. Hélary, E. Darque-Ceretti, and M. Aucouturier, J. Am. Ceram. Soc. **88**, 3218 (2005).
[6] A. Caiger Smith, *Luster Pottery* (New Amsterdam Books, New York, 1991).
[7] T. Pradell, J. Molera, J. Roque, A. D. Smith, D. Crespo, E. Pantos, and M. Vendrell, J. Am. Ceram. Soc. **88**, 1281 (2005).
[8] T. Pradell, J. Molera, C. Bayés, and P. Roura, Appl. Phys. A: Mater. Sci. Process. **83**, 203 (2006).
[9] T. Pradell, J. Molera, C. Bayés, P. Roura, and D. Crespo, J. Am. Ceram. Soc. (accepted).
[10] U. Kreijig and M. Vollmer, *Optical Properties of Metal Cluster*, Springer Series 25 (Springer, Berlin, 1995).
[11] S. Padovani *et al.*, Appl. Phys. A: Mater. Sci. Process. **79**, 229 (2004).
[12] G. Padeletti and S. Fermo, Appl. Phys. A: Mater. Sci. Process. **79**, 241 (2004).
[13] A. D. Smith, T. Pradell, J. Roque, J. Molera, M. Vendrell-Saz, A. J. Dent, and E. Pantos, J. Non-Cryst. Solids **352**, 5353 (2006).
[14] I. Farbman, O. Levi, and S. Efrima, J. Chem. Phys. **96**, 6477 (1992).
[15] B. Dusemund, A. Hoffmann, T. Salzmann, U. Kreibig, and G. Schmid, Z. Phys. D **20**, 305 (1991).
[16] J. Molera, M. Mesquida, J. Pérez-Arantegui, T. Pradell, and M. Vendrell, Archaeometry **43**, 455 (2001).
[17] T. Pradell, J. Molera, E. Pantos, A. D. Smith, C. M. Martin, and A. Labrador, Appl. Phys. A: Mater. Sci. Process. (accepted).
[18] A. Climent-Font, F. Pászti, G. García, M. T. Fernández-Jiménez, and F. Agulló, Nucl. Instrum. Methods Phys. Res. B **219–220**, 400 (2004).
[19] H. S. Cheng, H. Shen, J. Tang, and F. Yang, Nucl. Instrum. Methods Phys. Res. B **83**, 449 (1993).
[20] M. Mayer, SIMNRA User's Guide (IPP 9/113 1997); http://www.rzg.mpg.de/.
[21] W. K. Chu, J. W. Mayer, and M. A. Nicolet, *Backscattering Spectrometry* (Academic, New York, 1978).
[22] R. Jarjis, Key Eng. Mater. **132–136**, 1434 (1997).
[23] D. Hélary, PhD Thesis, Ecole des Mines de Paris, 2003.
[24] G. Padeletti, G. M. Ingo, A. Bouquillon, S. Pages-Camagne, M. Aucouturier, S. Roeres, and P. Fermo, Appl. Phys. A: Mater. Sci. Process. **83**, 475 (2006).
[25] J. Roqué, N. R. J. Poolton, J. Molera, A. D. Smith, E. Pantos, and M. Vendrell-Saz, Phys. Status Solidi B **243**, 1337 (2006).
[26] J. M. Fernández-Navarro, *El Vidrio*, 3rd ed. (CSIC, Madrid, 2003), Chap. IV, Sec. 10.
[27] S. Torquato, Phys. Rev. E **51**, 3170 (1995).
[28] J. J. Shiang, J. R. Heath, C. P. Collier, and R. J. Saykally, J. Phys. Chem. B **102**, 3425 (1998).
[29] V. Reillon and S. Bethier, Appl. Phys. A: Mater. Sci. Process. **83**, 257 (2006).
[30] R. B. Mason, *Shine Like the Sun. Luster-Painted and Associated Pottery from the Medieval Middle East*, Bibliotheca Iranica: Islamic Art and Architecture Series 12 (Mazda, Costa Mesa, Canada, 2004).